JOURNAL OF MATERIALS SCIENCE **34** (1999) 4519–4531

Preparation and characterisation of $MgSiN_2$ powders

R. J. BRULS, H. T. HINTZEN, R. METSELAAR
Centre for Technical Ceramics, Laboratory of Solid State and Materials Chemistry, Eindhoven University of Technology, P.O. Box 513, 5600 MB Eindhoven, The Netherlands
E-mail: R.j.BRULS@tue.nl

The powder preparation of $MgSiN_2$ was studied using several starting mixtures (Mg_3N_2/Si_3N_4, Mg/Si_3N_4 and Mg/Si) in the temperature range 800–1500 °C in N_2 or N_2/H_2 atmospheres. The phase formation was followed with TGA/DTA and powder X-ray diffraction (XRD). At 1250 °C Mg/Si mixtures did not yield single phase $MgSiN_2$ whereas for Mg/Si_3N_4 and Mg_3N_2/Si_3N_4 mixtures nearly single-phase powders were obtained. The Mg/Si_3N_4 mixtures yielded $MgSiN_2$ at the lowest processing temperature but the Mg_3N_2/Si_3N_4 mixtures yielded the most pure $MgSiN_2$ powder with respect to secondary phases. The main secondary phase detectable with XRD was MgO when starting from Mg_3N_2/Si_3N_4 or MgO and metallic Si when starting from Mg/Si_3N_4 mixtures. When the processing starting from Mg_3N_2/Si_3N_4 mixtures was optimised $MgSiN_2$ powders containing only 0.1 wt % O could be prepared. Using XRD the solubility of oxygen in the $MgSiN_2$ lattice was estimated to be at maximum 0.6 wt %. The $MgSiN_2$ powder was oxidation resistant in air till 830 °C. The morphology and particle size were studied with the scanning electron microscope (SEM) and the sedimentation method. Two different kinds of morphology were observed determined by the morphology of the Si_3N_4 starting material.

1. Introduction

As a consequence of the ever increasing miniaturisation of integrated circuits combined with a high energy dissipation, in recent years there is a strong need for substrate materials with improved thermal conductivity [1]. Because the electrical conductivity must be low, only non-metallic materials showing phonon conduction are suitable.

The traditional material Al_2O_3 does not longer fulfil the recent requirements. Several binary alternatives deduced from diamond, which has a high thermal conductivity and electrical resistivity, were considered [2], each material having its own disadvantages: SiC is electrically conducting, BeO is toxic, and the compound which is most intensively studied during the last years, viz. AlN, is considered to be expensive. Also the ternary compounds deduced from AlN were proposed e.g. $MgSiN_2$ (by replacing two Al^{3+} ions by a combination of Mg^{2+} and Si^{4+}) and Al_2OC (by replacing two N^{3-} ions by a combination of O^{2-} and C^{4-}) [3]. Recently, for $MgSiN_2$ ceramics a fairly high thermal conductivity was reported [4, 5].

For optimum thermal conductivity it is expected that the oxygen content of the $MgSiN_2$ ceramics should be low similar to that in AlN [6]. Therefore, for achieving $MgSiN_2$ ceramics with a high thermal conductivity the oxygen concentration of the starting material preferably should be low. In this paper we report about the preparation, phase formation and characterisation of $MgSiN_2$ powders with a low oxygen content. Preliminary results have already been published [7]. The present situation concerning the preparation of ceramic samples and thermal conductivity is described elsewhere [8].

2. Experimental

2.1. Starting materials

$MgSiN_2$ powders were prepared from Mg_3N_2/Si_3N_4, Mg/Si_3N_4 or Mg/Si powder mixtures. The influence of the composition and impurity content (quality) of various starting materials on the characteristics of the resulting $MgSiN_2$ powders was investigated for Mg_3N_2 (Table I) and Si_3N_4 (Tables II and III). Mg powder of Merck (5815) and Si powder of Riedel de Haen AG were used.

2.2. Preparation

The starting materials were mixed in stoichiometric amounts in a glove-box to prevent oxidation and hydrolysis of the starting materials, especially Mg_3N_2. Subsequently, the mixed powders were put in a closed stainless steel (AISI 304) tube. When further purification of the resulting powders became necessary, molybdenum (Plansee, regular grade) tubes were used. The tubes had a small gas inlet/outlet to prevent pressure built up. The starting mixtures were normally fired at 1250 °C during 16 h in a horizontal tube furnace in

TABLE I Characteristics of the used Mg_3N_2 starting materials (data from the supplier)

Manufacturer	Code	[N] (wt %)	[N + Mg] (wt %)
Alfa	932825	27.4	99.5
Cerac	M1014	26.0	99.5
Theoretical	—	27.8	100

TABLE II Characteristics of the used Si_3N_4 starting materials (data from this work)

Manufacturer	Code	$[N]^a_{meas}$ (wt %)	$[N]_{spec}$ (wt %)	$[O]^b_{meas}$ (wt %)	$[O]_{spec}$ (wt %)
SKW Trostberg	Silzot HQ	38.7 ± 0.3^b	>38.5 (38.74[c])	0.7 ± 0.1	<1.0 (0.34[c])
Cerac	S1177	38.4 ± 0.4	>38.0	0.7 ± 0.1	
HCST	LC12N	39.2 ± 0.1	>38.5	1.4 ± 0.1	1.4–1.7
Kema Nord	—	38.4 ± 0.3	—	2.4 ± 0.1	
Sylvania	—	29.5 ± 0.3	—	4.1 ± 0.2	
Tosoh	TS10	39.3 ± 0.5	—	1.6 ± 0.1	
Ube	SNE10	37.7 ± 0.6	>38.0	1.2 ± 0.1	<2.0
Theoretical		39.9		0	

[a] Measured with Kjeldahl method.
[b] Measured with the LECO O/N gas-analyzer.
[c] Data given by supplier.

a flowing N_2 (99.95% pure) or 85 vol % N_2 (99.95% pure)/15 vol % H_2 (99.95% pure) atmosphere. The firing temperature of 1250 °C was taken from two earlier studies on the preparation of $MgSiN_2$ [4, 9]. Also other firing temperatures in the range of 900–1500 °C were used.

2.3. Characterisation

The starting powders and the powders resulting after firing the starting materials were characterised with powder X-ray diffraction (XRD, Philips PW 1050/25, CuK_α). The Mg_3N_2 and Si_3N_4 starting materials were characterised in the range of 10°–100° respectively 10°–80° 2Θ using a scan rate of 1°/min respectively 2°/min. The phase formation of the fired materials was investigated with powder X-ray diffraction. They were investigated in the range of 10°–100° 2Θ using standard continuous scans (1° or 2°/min) as well as step scans (0.1°/min).

The lattice parameters of $MgSiN_2$ were calculated with the computer program Refcel [10] using the fact that $MgSiN_2$ has an orthorhombic cell (space group $Pna2_1$ [11]). At least ten reflections (200, 002, 121, 201, 122, 202, 040, 320, 123, 203, 042, 241, 322, 401, 242 and 243) including a zero point correction were used for calculating the lattice parameters.

The nitrogen content of the Si_3N_4 starting materials was determined by the Kjeldahl method or the LECO TC 436 O/N analyser. For the first method the sample (0.1 g powder) was decomposed in molten LiOH. The releasing ammonia was binded in a saturated boric acid solution. The amount of ammonia was determined by titration with 0.1M hydrochloric acid using bromophenolblue as indicator. For the second method the nitrogen present in the sample was thermally converted at high temperatures to N_2 which is measured with a catharometer.

The oxygen content for the Si_3N_4 starting materials and the $MgSiN_2$ powders was measured using a LECO TC 436 O/N analyser. The powder sample was mixed with carbon whereafter the oxygen present in the sample is carbothermally converted at high temperatures in an inert atmosphere into CO, which after further oxidation to CO_2 is measured with IR-absorption spectroscopy.

Thermal analysis TGA/DTA was performed with a Netzsch STA 409 thermobalance to investigate the phase formation and oxidation of $MgSiN_2$. The phase formation was studied in flowing N_2 atmosphere using Al_2O_3 sample holders applying a constant heating rate of 10°/min. The oxidation study was performed in flowing air using Al_2O_3 sample holders applying a constant heating rate of 5°/min. Also tube furnace oxidation experiments in air were performed in combination with XRD and mass measurements to determine the (intermediate) reaction products and to study the oxidation kinetics.

Scanning electron microscopy (SEM, JEOL 840A) was used to study the particle size and morphology of some of the prepared powders, and energy dispersive spectrometry (EDS) to determine the chemical composition of the powders, especially the presence of contamination(s).

The particle size distribution was measured with a Sedigraph 5100 Micromeritrics using a 60 wt % ethylene glycol/40 wt % water mixture. Before measuring the particle size distribution the dispersed powder mixture was ultrasonic treated for 20 min to break up powder agglomerates.

TABLE III Characteristics of the used Si_3N_4 starting materials (data from this work)

Manufacturer	Code	$\left(\frac{\alpha}{\alpha+\beta}\right)_{meas}$	$\left(\frac{\alpha}{\alpha+\beta}\right)_{spec}$	$(d_{50})_{spec}$ (μm)	$(d_{50})_{meas}$ (μm)	$(d_{90})_{meas}$ (μm)
SKW Trostberg	Silzot HQ	0.66	>0.80	1.7	2.2	4.9
Cerac	S1068	0.08	±0.1	<2.0	1.2	2.6
HCST	LC12N	0.89[a]	0.94	0.6	0.6	3.0
Kema Nord	—	0.91[a]	—	—	2.3	9.0
Sylvania	—	Amorphous	Amorphous	—	—	—
Tosoh	TS10	0.93	—	—	1.1	7.5
Ube	SNE10	1.00[a]	>0.95	0.6	0.7	1.4

[a] Also some Si_3N_4 with the tetragonal modification present.

3. Results and discussion

3.1. Starting powder characteristics

3.1.1. Mg_3N_2

At maximum 0.5 wt % of impurities are present in the Mg_3N_2 starting materials (Table I). The significant difference between the nitrogen concentration given by the supplier for Mg_3N_2 from Cerac (26.0 wt %) and the expected value (27.8 wt %) gives evidence for the presence of free magnesium metal. The major impurity is oxygen which is present as MgO as observed with XRD. During the reaction of Mg metal with Si metal in a flowing nitrogen atmosphere an Mg_3N_2 ceramic disk ($\varnothing \approx 20 \times 0.4$ mm) was formed. This disk was also investigated with XRD using the same conditions as for the investigated Mg_3N_2 powders. Almost no MgO could be detected in this sample with XRD.

Because Mg_3N_2 has a cubic lattice it is possible to calculate the true lattice parameter by plotting the lattice parameter a calculated for each reflection versus the function $f(\Theta)$, which is given by:

$$f(\Theta) = \frac{\cos^2(\Theta)}{\sin(\Theta)} + \frac{\cos^2(\Theta)}{\Theta}$$

and extrapolating to $f(\Theta) = 0$ (see Ref. [12]). In Fig. 1 the lattice parameter, a, for each reflection of the Mg_3N_2 starting powders and the ceramic Mg_3N_2 disk is plotted versus $f(\Theta)$. For comparison data of the JCPDS card 35-778 concerning Mg_3N_2 powder (Cerac) are also included. From this figure it can be deduced that, although severe differences occur for the lattice parameters calculated from the individual reflections, the extrapolated lattice parameter for all samples is the same viz. 9.963 ± 0.002 Å, which is comparable with the lattice parameter mentioned in JCPDS card 35-778 (9.9657 Å). Because the lattice parameter was the same for all investigated Mg_3N_2 samples and the impurity content of the powder samples was at maximum 0.5 wt % it can be concluded that the Mg_3N_2 lattice is saturated with oxygen and that the solubility of oxygen in the Mg_3N_2 lattice is very low.

3.1.2. Si_3N_4

In Tables II and III the measured powder characteristics of the used Si_3N_4 powders are presented. The nitrogen content measured for all investigated Si_3N_4 powders is in good agreement with the specification of the suppliers. The oxygen concentration in the Si_3N_4 starting materials ranges from 0.7 to 4.1 wt %. For the SKW Trostberg Si_3N_4 powder the measured oxygen content (0.7 wt %) is well within the specifications but considerably higher than the content measured by the supplier (0.34 wt %). It can be seen that for materials with a nitrogen concentration close to the theoretical value (>39 wt %), the oxygen concentration is low. A considerable deviation of the nitrogen concentration from the theoretical value combined with a low oxygen content was measured for the Cerac, Ube and SKW Trostberg Si_3N_4 powders. This indicates that some free silicon or silicon containing compound like SiC may be present. According to the supplier is for the SKW Trostberg Si_3N_4 the free Si metal content smaller than 0.5 wt % but some SiC (0.4 wt %) is present.

The crystallographic modification of the Si_3N_4 powders, viz. amorphous, α (JCPDS card 41-360), β (JCPDS card 33-1160) or tetragonal phase (JCPDS card 40-1129), was determined with XRD. For the crystalline powders the $\alpha/\alpha+\beta$ ratio was calculated (Tables II and III) using the methods described in Ref. [13]. The calculated $\alpha/\alpha+\beta$ ratio agrees quite well with the specification of the suppliers. Only the measured $\alpha/\alpha+\beta$ ratio of SKW Trostberg Si_3N_4 deviates about 15% from the specified ratio.

For all investigated Si_3N_4 powders the median particle size, d_{50}, was less than 2.5 μm (Tables II and III) and some are submicron (Ube and HCST). The Si_3N_4 powders of HCST, Kema Nord and Tosoh have a broad particle size distribution ($3 \times d_{50} < d_{90}$) which

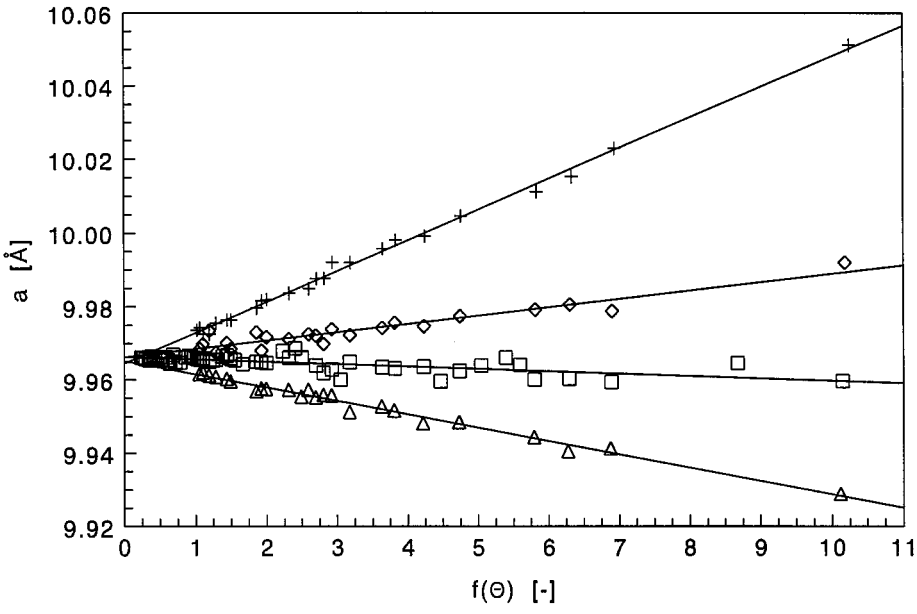

Figure 1 Cubic lattice parameter a of Mg_3N_2 powder of Cerac (+), Alfa (◇), JCPDS 35-778 (□), and Mg_3N_2 ceramic disk (△) as a function of $f(\theta)$.

indicates that the primary particles are most probably agglomerated, even after ultrasonic treatment.

3.2. Phase formation of $MgSiN_2$

The TGA/DTA experiments show that when starting with an Mg_3N_2/Si_3N_4 mixture the temperature should surpass about 1100–1150 °C to get fast formation of $MgSiN_2$, in agreement with literature data [9]. In the DTA signal two endothermic peaks are present. Which peak or whether both peaks can be ascribed to the formation of $MgSiN_2$ is not clear because both peaks are less than 50 °C separated from each other. No attempts were made to discriminate between them because the used standard synthesis temperature of 1250 °C is sufficiently high to obtain a fast reaction and a fully reacted product.

For the Mg/Si_3N_4 starting mixture, the reaction mechanism is much more complicated than for the previous case. Several exothermic DTA peaks are present (Fig. 2), the strongest at 612 °C, and some smaller ones at 897, 920 and 1061 °C (not visible in Fig. 2). At about 612 °C nitridation of Mg takes place accompanied by a mass gain of about 9.5 wt %. The total mass gain at 1000 °C is about 12.5 wt % which is comparable with the expected mass gain of 13.1 wt % for the nitridation of the Mg present in the Mg/Si_3N_4 starting mixture. XRD showed that a Mg/Si_3N_4 mixture fired at 700 °C in an N_2 atmosphere resulted in a mixture of Mg_3N_2 and Si_3N_4 whereas a mixture fired at 900 °C resulted in $MgSiN_2$ giving further evidence that the DTA signals at 897 and 920 °C are related with the formation of $MgSiN_2$.

Also the nitridation of metallic Mg powder was studied with TGA/DTA. At 648 °C an endothermic peak is observed which can be ascribed to the melting of Mg metal. Two exothermic nitridation peaks were observed at 660 and 690 °C. The last one is related to the rapid nitridation of Mg. The observed results are in good agreement with earlier published data [14] on the nitridation of Mg. When these results are compared with those obtained for the Mg/Si_3N_4 mixtures, a lowering by about 50 °C of the nitridation temperature of Mg and no melting peak of Mg is observed when using the Mg/Si_3N_4 mixtures. A possible explanation might be a different reactivity of Mg in the presence of Si_3N_4.

When comparing the phase formation of $MgSiN_2$ starting with Mg_3N_2/Si_3N_4 and Mg/Si_3N_4 mixtures it can be concluded that when starting with an Mg/Si_3N_4 mixture nearly single-phase $MgSiN_2$ can already be obtained at a temperature of about 900 °C, which is much lower than the minimal temperature of about 1150 °C necessary for an Mg_3N_2/Si_3N_4 mixture. This difference in phase formation temperature might be related to the fact that during nitridation of Mg an Mg_3N_2 phase is formed different from the room temperature modification [15] with a higher reactivity. Also gas phase reactions may play an important role in the observed difference in temperature. When Mg(g) condenses on the Si_3N_4 particles the reactivity of the starting mixture might be increased resulting in a lower reaction temperature.

In order to study the observed differences between the Mg_3N_2/Si_3N_4 and Mg/Si_3N_4 starting mixtures in more detail the phase formation of $MgSiN_2$ for several Mg_3N_2/Si_3N_4 fired at 1250 °C and for Mg/Si_3N_4 starting mixtures fired at 900–1250 °C using different starting materials was studied with XRD. For completeness also the phase formation for a Mg/Si starting mixture at 1250 °C was studied.

Nearly single-phase grey-brown coloured $MgSiN_2$ materials were obtained when starting with Mg_3N_2/Si_3N_4 mixtures fired at 1250 °C or Mg/Si_3N_4 mixtures fired at 900–1250 °C in an N_2 atmosphere. For all Si_3N_4 starting materials (amorphous, α or β modification, irrespective of the presence of tetragonal phase or free Si), $MgSiN_2$ is readily formed. In all cases some MgO (periclase, JCPDS card 4-829) could be detected with XRD as a secondary phase. Sometimes white powder was observed at the outside of the reaction tube. This

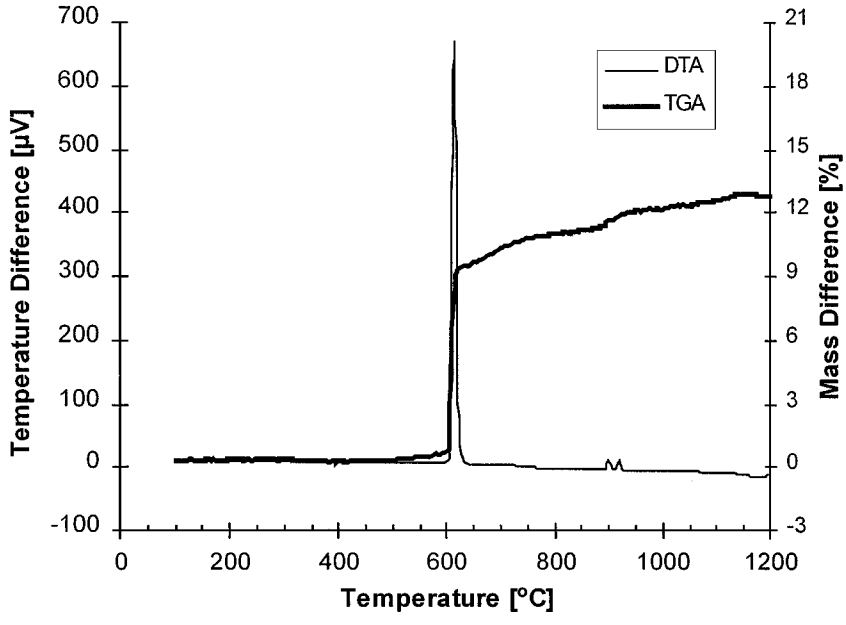

Figure 2 TGA/DTA plot of an Mg/Si_3N_4 mixture in a nitrgen atmosphere.

powder was also MgO, as observed with XRD, indicating that the oxygen in the starting materials or the gas atmosphere reacts with Mg or Mg_3N_2 to MgO. The MgO contamination is caused by oxygen impurities in the starting material and oxygen pickup during the processing (mixing) and the synthesis (oxygen impurities in the N_2 atmosphere/reaction with oxides from the stainless steel tubes).

The relative MgO content (I/I_0) in the $MgSiN_2$ powders was determined by dividing the intensity of the strongest reflection of MgO ($hkl = 200$) by the intensity of the strongest reflection of $MgSiN_2$ ($hkl = 121$) multiplied by 100. As expected the observed MgO content decreases for the purer Si_3N_4 starting materials. Almost no MgO could be detected ($I/I_0 = 3$) for the Mg_3N_2/Si_3N_4 and Mg/Si_3N_4 mixtures using oxygen poor Si_3N_4 starting powders of SKW Trostberg and Cerac respectively. In general for the same Si_3N_4 starting material the least amount of MgO was observed when using Mg instead of Mg_3N_2 indicating that the purity of the resulting $MgSiN_2$ might be improved by using a Mg/Si_3N_4 instead of a Mg_3N_2/Si_3N_4 mixtures.

Another advantage of using Mg/Si_3N_4 mixture is that, due to the lower firing temperature necessary, a less non stoichiometric product, caused by possible evaporation of magnesium [4], will be formed. Other possible additional advantages of a lower firing temperature may be less contamination of the prepared materials with metals from the stainless steel (or molybdenum) tubes, and a smaller particle size which will improve the sinterability of the resulting powders. So using Mg/Si_3N_4 instead of Mg_3N_2/Si_3N_4 starting mixtures might be beneficial for preparing a pure $MgSiN_2$ powder because the reaction temperature can be lowered. However, in the powders synthesised from Mg/Si_3N_4 mixtures always some free Si metal (JCPDS 27-1402) was detected with XRD. So, Mg cannot only react with the N_2 atmosphere forming Mg_3N_2 but also with the Si_3N_4 powder forming Mg_3N_2 and metallic Si [11]. Because the nitridation of metallic Si is kinetically hampered even at the standard processing temperature of 1250 °C [16] removing of this secondary phase is a problem. So, the advantages of the lower reaction temperature when using Mg/Si_3N_4 mixtures are cancelled by the reaction of Mg with Si_3N_4 forming metallic Si which cannot be removed at low reaction temperatures.

Starting with an Mg/Si mixture in a stainless steel reaction tube fired in a flowing N_2 atmosphere at 1250 °C $MgSiN_2$ was formed. However, in this case no single-phase $MgSiN_2$ was obtained. The black coloured reaction product consisted mainly of $MgSiN_2$ and several not identified secondary phases. In the coldest part of the reaction tube a light brown-orange coloured ceramic disk was formed. This disk ($Ø \approx 20 \times 0.4$ mm) was investigated with XRD. It was concluded that Mg condensed in the coldest part of the reaction tube as Mg_3N_2 ceramic. Considering those difficulties, no further attempts were made to obtain single-phase $MgSiN_2$ powder using a Mg/Si starting mixture.

In summary the phase formation study at 1250 °C using Mg_3N_2/Si_3N_4, Mg/Si_3N_4 and Mg/Si starting mixtures showed that only the first two starting mixtures resulted in nearly single phase $MgSiN_2$. Although the TGA/DTA and furnace experiments indicate that $MgSiN_2$ can be synthesised at 900 °C using Mg/Si_3N_4 starting mixtures, the use of a Mg_3N_2/Si_3N_4 starting mixture at 1250 °C is preferred because the resulting $MgSiN_2$ powder contains less Si impurities. In general when a molybdenum tube was used instead of a stainless steel tube the resulting $MgSiN_2$ powder had a much more homogeneous and lighter colour indicating that the powder contained less metallic contaminations (Fe, Cr and Ni as detected with SEM/EDS). Based on the MgO found at the outside of the reaction tube it can be assumed that MgO(g) can evaporate from the starting mixture. Using these results it was tried to synthesise an oxygen poor $MgSiN_2$ powder.

For this we used the Mg_3N_2/Si_3N_4 starting mixture with the lowest oxygen content (Mg_3N_2(Alfa)/Si_3N_4 (SKW Trostberg)). If the oxygen of the MgO at the outside of the reaction tube originates from the starting mixture then it is possible to purify the resulting $MgSiN_2$ powder by adding an excess amount of Mg or Mg_3N_2 to the starting mixture. The starting powder, with a small excess of Mg_3N_2 (±1 wt %) intentionally added, was fired in a 50 ml/h N_2 (99.995% pure)/5 ml/h H_2 (99.9999% pure) atmosphere for 3 h at 1250 °C and subsequently 1 h at 1500 °C in a molybdenum tube using a heating and cooling rate of 3 °C/min. The excess of Mg_3N_2 is used for maintaining the stoichiometry in the resulting $MgSiN_2$ powder. The heat treatment at 1500 °C was performed to ensure that the starting materials had fully reacted, to nitridate possible metallic Mg and Si impurities in the starting powders, to evaporate the MgO present in the reaction mixture and to remove the Mg_3N_2 excess present in the reaction product by decomposition into Mg(g) and N_2 [17]. So the stoichiometry of the reaction product is maintained because $MgSiN_2$ is stable at 1500 °C [17] and the added excess of Mg_3N_2 which did not react to MgO is also removed from the reaction mixture.

Using this procedure single phase white $MgSiN_2$ powder was formed. With XRD using a scan rate of 0.033°/min only a small trace of MgO ($I/I_0 = 0.4$) could be detected. This indicates that the excess Mg_3N_2 does not increase the MgO content in the resulting $MgSiN_2$ powder under the given reaction conditions. Because also no Mg_3N_2 could be detected this indicates that during the reaction Mg_3N_2 or Mg_3N_2 and MgO evaporates from the reaction mixture.

3.3. Oxygen content of the $MgSiN_2$ powders

The oxygen content of the $MgSiN_2$ powders synthesised at 1250 °C is presented in Table IV. The influence of the reaction temperature, in the range of 1000–1250 °C, on the oxygen content of the resulting $MgSiN_2$ powders was negligible. As expected, the overall oxygen content becomes lower when using purer Si_3N_4 starting materials. Also, using Mg_3N_2 from Alfa (with the highest nitrogen content, Table I) instead of Mg_3N_2 from Cerac decreases the oxygen content of the synthesised $MgSiN_2$ powder. Use of Mg instead

TABLE IV Overall oxygen content of the $MgSiN_2$ powders prepared from different starting materials at 1250 °C in wt %

Starting materials		Mg_3N_2		Mg-metal
Si_3N_4	[O] (wt %)	Cerac	Alfa	Merck
SKW Trostberg	0.3–0.7	—	0.9	—
Cerac	0.7	1.4	1.0	1.0
Ube	1.2	—	1.6	—
HCST	1.4	—	1.6	1.3
Tosoh	1.6	2.0	1.7	1.5
Kema Nord	2.4	3.0	2.2	2.8
Sylvania	4.1	5.3	6.1	3.9

of Mg_3N_2 as a starting material results in an even somewhat lower oxygen concentration in the $MgSiN_2$ powder. However, if the oxygen content in the used Si_3N_4 starting material is low the difference in the oxygen content of $MgSiN_2$ starting from Mg_3N_2/Si_3N_4 or Mg/Si_3N_4 mixtures appears to be negligible. So the oxygen content of the Si_3N_4 starting material is the dominating factor. For the standard synthesis temperature of 1250 °C the lowest oxygen content of about 0.9–1.0 wt % is obtained for the purest Si_3N_4 starting materials (Cerac S1068 and SKW Trostberg Silzot HQ). It is significantly below the value of about 4 wt % obtained in a previous study [4].

Fig. 3 shows the relative MgO content of the $MgSiN_2$ powders synthesised at 1250 °C as a function of the overall oxygen content. When the oxygen content is high (>2 wt %), no strong correlation between the relative MgO content and the oxygen content is observed because the oxygen can be present in several secondary phases. Whereas, in case the oxygen content is low (≤2 wt %), a correlation is observed. Assuming that MgO is the only oxygen containing component at overall oxygen concentrations ≤2 wt %, a crude estimation of the maximum solubility of oxygen in the $MgSiN_2$ lattice was made by extrapolation to a relative MgO content equalling 0, yielding a maximum oxygen concentration of about 0.6 ± 0.2 wt %. Above this solubility limit oxygen MgO is formed as a secondary phase, whereas below this limit oxygen is assumed to incorporate in the $MgSiN_2$ lattice. The maximum solubility of 0.6 wt % oxygen in the $MgSiN_2$ lattice corresponds to 0.6×10^{21} O/cm^3 at maximum, as compared with about 6×10^{21} O/cm^3 reported for AlN [3]. So the solubility of oxygen in the $MgSiN_2$ lattice is much lower than in AlN.

The $MgSiN_2$ powder synthesised using the purest starting materials by firing first at 1250 and subsequently at 1500 °C contained only 0.1 ± 0.1 wt % O as determined with the LECO gas analyser. This value is considerably lower than that measured for the $MgSiN_2$ powder synthesised at 1250 °C using the same starting materials (0.9 wt % O). This value is even lower than the value expected from the oxygen content of the used starting mixture (∼0.6 wt % O) indicating that during the synthesis the oxygen content in the reaction mixture decreases. The unexpected low oxygen content might be caused, as discussed before, by a (partially) reaction of the weighed-out Mg_3N_2 with the oxygen present in the starting mixture to MgO which evaporates from the reaction mixture. An additional effect might be the carbothermal nitridation reaction occurring at the higher firing temperature between the trace SiC, present in the SKW Trostberg Si_3N_4 starting powder, and the oxygen containing compounds present in the starting mixture.

The low oxygen content in combination with the fact that still some MgO was detectable with XRD ($I/I_0 = 0.4$) indicates that the maximum solubility of oxygen in the $MgSiN_2$ lattice is most probably well below the estimated 0.6 wt % based on Fig. 3. So the estimation of the maximum solubility of oxygen in the $MgSiN_2$ lattice might be conservative.

The $MgSiN_2$ powder sample with the low oxygen content of 0.1 wt % contained 34.2 ± 1.7 wt % N which is considerably higher than the value obtained

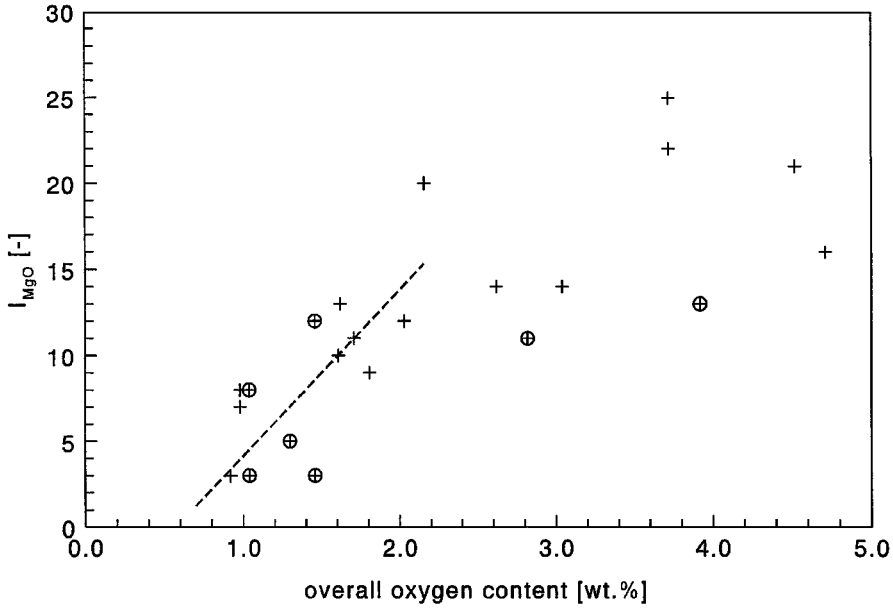

Figure 3 The relative MgO content (as determined from the 200 reflection by XRD) of several $MgSiN_2$ powders synthesised at 1250 °C from Mg_3N_2/Si_3N_4(+) and Mg/Si_3N_4(⊕) mixtures as a function of the overall oxygen content (as determined with the LECO O/N gas-analyser).

TABLE V List of d-values and relative intensities of pure $MgSiN_2$ evaluated from ceramic samples

hkl value	$\bar{d}_{obs}$ [Å]	d_{obs} [Å]	$\overline{I/I}_{0,obs}$	d-value according JCPDS 25–530 [Å]	I/I_0 according to JCPDS 25–530
110	4.09	4.08	9	4.1	12
011	3.949	3.945	10	3.96	14
111	3.160	3.158	1	3.14	8
120	2.758	2.756	88	2.76	85
200	2.6349	2.6332	45	2.642	55
002	2.4922	2.4907	80	2.496	100
210	2.4405	2.4384	3		
121	2.4133	2.4113	100	2.415	95
201	2.3294	2.3283	23	2.336	30
211	2.1919	2.1909	1		
112	2.1278	2.1258	1		
220	2.0434	2.0426	<1		
130	1.9969	1.9952	<1		
031	1.9803	1.9792	3	1.983	3
221	1.8907	1.8909	<1		
122	1.8491	1.8483	28	1.850	30
202	1.8106	1.8098	12	1.811	18
212	1.7437	1.7429	2		
310	1.6953	1.6947	2		
040	1.6184	1.6185	25	1.621	20
013	1.6093	1.6089	1		
231	1.5830	1.5826	1		
132	1.5584	1.5578	1		
140	1.5471			1.549	45
320	1.5439	1.5436	36		
141	1.4775			1.482	3
321	1.4748	1.4745	1		
123	1.4232	1.4228	34	1.425	40
203	1.4054	1.4051	11	1.409	18
240	1.3790	1.3786	7	1.381	10
213	1.3734	1.3740	1		
042	1.3573	1.3569	15	1.359	16
241	1.3291	1.3288	11	1.328	12
400/033	1.3175/1.3164	1.3173	1		
322	1.3125	1.3122	22	1.314	30
401	1.2737	1.2735	5	1.275	8
150	1.2573	1.2569	1		
051	1.2531	1.2526	1		
004	1.2461	1.2458	2	1.248	5
420	1.2202	1.2201	<1		
151	1.2191	1.2186	<1		
242	1.2066	1.2063	5	1.208	7
332	1.1954	1.1950	<1		
114	1.1919	1.1918	1		
313/421	1.1866/1.1852	1.1868	<1		
233	1.1776	1.1773	1		
402	1.1647	1.1643	1		
124	1.1356	1.1353	2	1.133	3
251	1.1317	1.1309	1		
204	1.1265	1.1262	1	1.129	2

in a previous study (30.7 wt % [4]), and only somewhat lower than theoretical value (34.8 wt %). This is in agreement with the fact that due to the presence of some residual oxygen and possibly other contaminations, the nitrogen content should be somewhat lower than the theoretical value.

3.4. X-ray diffraction data of $MgSiN_2$

From the present XRD study of $MgSiN_2$ powders and another study of $MgSiN_2$ ceramics [18] we know that the indexing of the $MgSiN_2$ reflections given in JCPDS card 25-530 is not completely correct. The data of ceramic samples were used to revise the published XRD data of $MgSiN_2$ powders because the ceramic samples gave a better signal-noise ratio than the powder samples. The revised data (Table V) were obtained from $MgSiN_2$ ceramic samples [18] with an average grain size of 0.25–1.5 μm in which no preferential orientation was detectable with XRD using a cylindrical camera. The data were used to identify the powder samples. The d-values, $\bar{d}_{obs}$, presented are calculated using the average observed lattice parameters (orthorhombic lattice $a = 5.2698 \pm 0.0013$, $b = 6.4736 \pm 0.0014$ and $c = 4.9843 \pm 0.0010$ Å) determined for several ceramic samples. The relative intensities, $\overline{I/I}_{0\,obs}$ are the average measured relative intensities for those ceramic samples. For determining the lattice parameters the computer program Refcel with zero point correction was used taking into account at least ten reflections. For comparison an observed d-value list (d_{obs}) of

a ceramic sample is included in Table V and also the data of JCPDS card 25-530 of $MgSiN_2$, which refers to the results of David [19], are presented.

As can be seen from Table V the d-value list of $MgSiN_2$ was revised by adding some low intensity peaks which are not mentioned in JCPDS card no. 25-530. We especially mention the 210 ($d = 2.4405$ Å), 212 ($d = 1.7437$ Å) and 310 ($d = 1.6953$ Å) reflections because they have a relative strong intensity ($I/I_0 \approx 2 - 3$) as compared to the other low intensity peaks ($I/I_0 \leq 1$) which were added. Another difference is that in JCPDS card no. 25-530 the d-values 1.549 and 1.482 Å are indexed with $hkl = 140$ and 141 whereas we indexed these reflections as 320 and 321, respectively. Furthermore, some differences in observed intensity I/I_0 are noticed, especially for the 111 reflection for which $I/I_0 = 8$ according to JCPDS 25-530 whereas we observed a much lower value of $I/I_0 = 1$.

However, David *et al.* [11] calculated a theoretical intensity of $I/I_0 = 0.7$ [11], which is in excellent agreement with the intensity of $I/I_0 = 1$ observed by us. This mismatch in calculated and measured intensity by David *et al.* is tentatively ascribed by us to the presence of free Si (JCPDS card 27-1402) in their $MgSiN_2$ powder, which increased the intensity measured for the 111 reflection. The 111 reflections of Si and $MgSiN_2$ have similar d-values of 3.136 and 3.160 Å respectively.

The indexation of the 140 and 141 reflections was changed because if a synthetic pattern (d-value list of all possible reflections) was generated using calculated lattice parameters, the d-value of the 320 and 321 reflection matched much better the experimentally found d-values than the calculated d-value of the 140 and 141 reflection. As an example the d-values observed for a ceramic $MgSiN_2$ sample, d_{obs}, can be compared with the calculated d-values using the average lattice parameters, $\bar{d}_{obs}$, determined from the ceramic samples (Table V). Using the atomic positions for $MgSiN_2$ taken from Ref. [20] and a computer program for calculating X-ray diffraction intensities (Powder Cell [21]) we also concluded that the 140 and 141 reflection should indeed be replaced by the 320 and 321 reflection, respectively. The intensity calculated for the 140 and 141 reflection is $\ll 1$ whereas the calculated intensity of the 320 and 321 reflection were in good agreement with the measured intensity. Furthermore David *et al.* [11] calculated a much higher intensity for the 320 than for the 140 reflection (49.7 vs. 0.1 respectively) whereas the calculated intensity of the 141 matched better than the one calculated for the 321 reflection (3.4 vs. 0.4 respectively). Also Wild *et al.* [22] used the 320 reflection instead of the 140 reflection.

From the plots of the lattice parameters measured for the $MgSiN_2$ powders processed at 1250 °C vs. the measured overall oxygen content and the cell volume vs. the measured overall oxygen content it was concluded that the samples have the same lattice parameters ($a_{average} = 5.275 \times 0.007$, $b_{average} = 6.472 \times 0.009$ and $c_{average} = 4.987 \times 0.011$ Å) and cell volume ($V_{average} = 170.25 \pm 0.70$ Å^3). So, the lattice parameters and cell volume of the samples processed at 1250 °C was independent of the oxygen content. As an example, in Fig. 4 the unit cell volume measured for the $MgSiN_2$ powders processed at 1250 °C is presented as a function of the measured overall oxygen content. The error bar indicated in Fig. 4 equals 3 times the calculated standard deviation for the Refcel unit cell volume calculation. Within the limits of accuracy the results are in agreement with the lattice parameters used in Table V for the ceramic samples. Because the lattice parameters for all samples synthesised at 1250 °C are the same irrespective of the overall oxygen content ranging from 0.9–6.1 wt % it is concluded that the maximum solubility of oxygen in the $MgSiN_2$ lattice is surpassed. This is in accordance with the estimated maximum oxygen solubility of 0.6 wt % in the $MgSiN_2$ lattice; therefore no influence of the overall oxygen concentration on the lattice parameters is expected above 0.6 wt % oxygen.

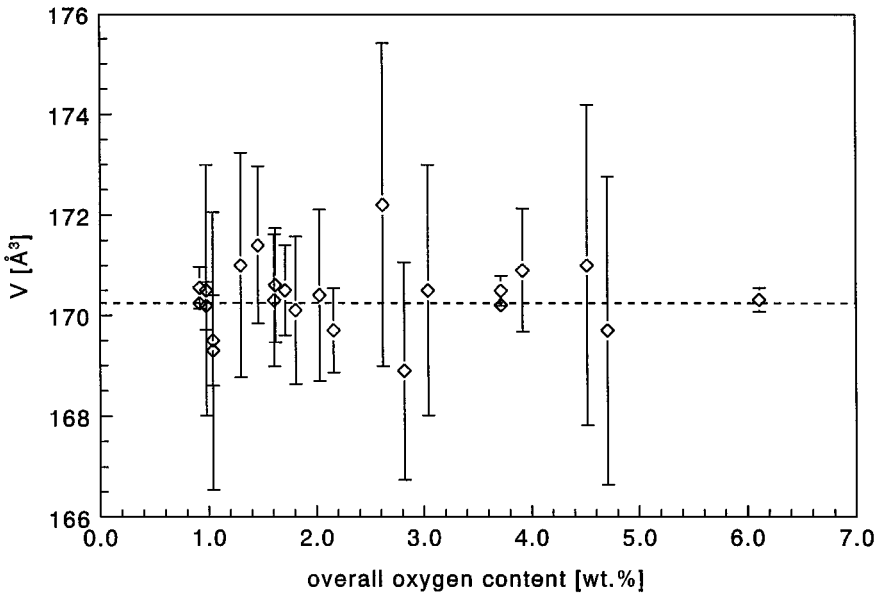

Figure 4 The calculated cell volume determined for several $MgSiN_2$ powders versus the measured oxygen content.

For the $MgSiN_2$ powder with an oxygen content of about 0.1 wt %, first fired at 1250 and subsequently 1500 °C, the lattice parameters are $a = 5.276 \pm 0.006$, $b = 6.477 \pm 0.006$ and $c = 4.990 \pm 0.005$ Å. This is comparable with the calculated average lattice parameters observed for the ceramic and powder samples indicating that the solubility of oxygen is most probably even less than 0.1 wt % O.

3.5. Powder characteristics

The morphology and particle size as observed with SEM is similar for $MgSiN_2$ powders prepared from Mg_3N_2/Si_3N_4 and Mg/Si_3N_4 mixtures when the same Si_3N_4 starting material is used (Figs 5 and 6). This was confirmed by sedigraph measurements of $MgSiN_2$ powders prepared from Mg_3N_2/Si_3N_4 and Mg/Si_3N_4 mixtures. The $MgSiN_2$ powder prepared from Mg has a

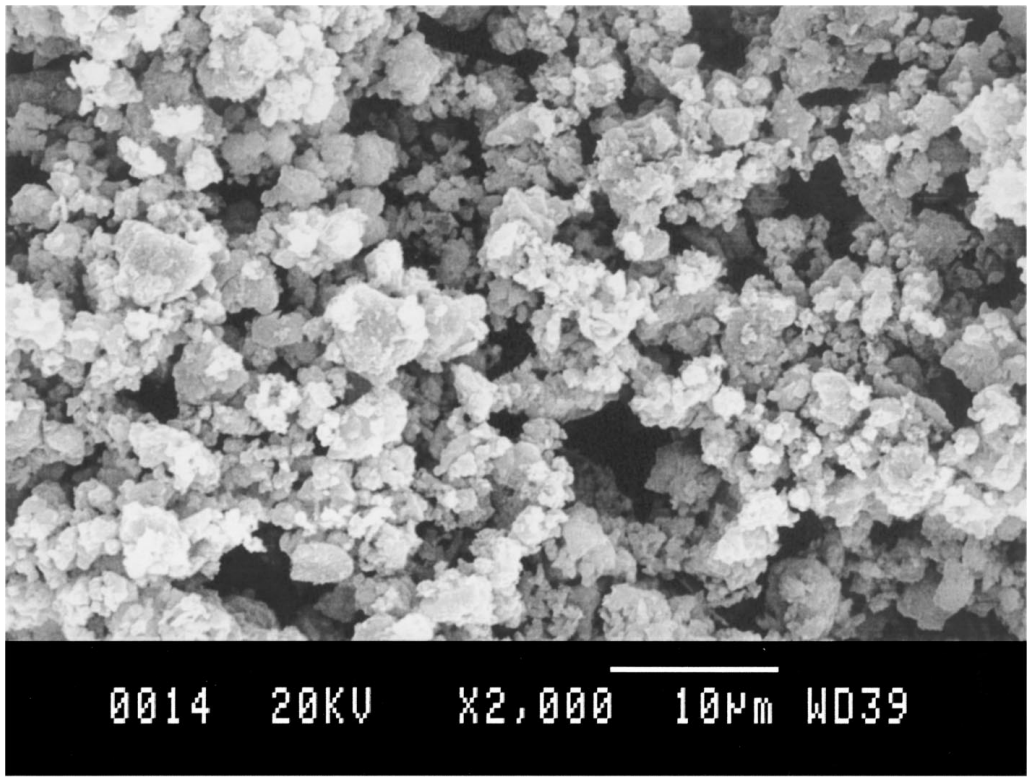

Figure 5 SEM picture of an $MgSiN_2$ powder synthesised at 1250 °C from a Si_3N_4 (SKW Trostberg)/Mg_3N_2 (Alfa) starting mixture.

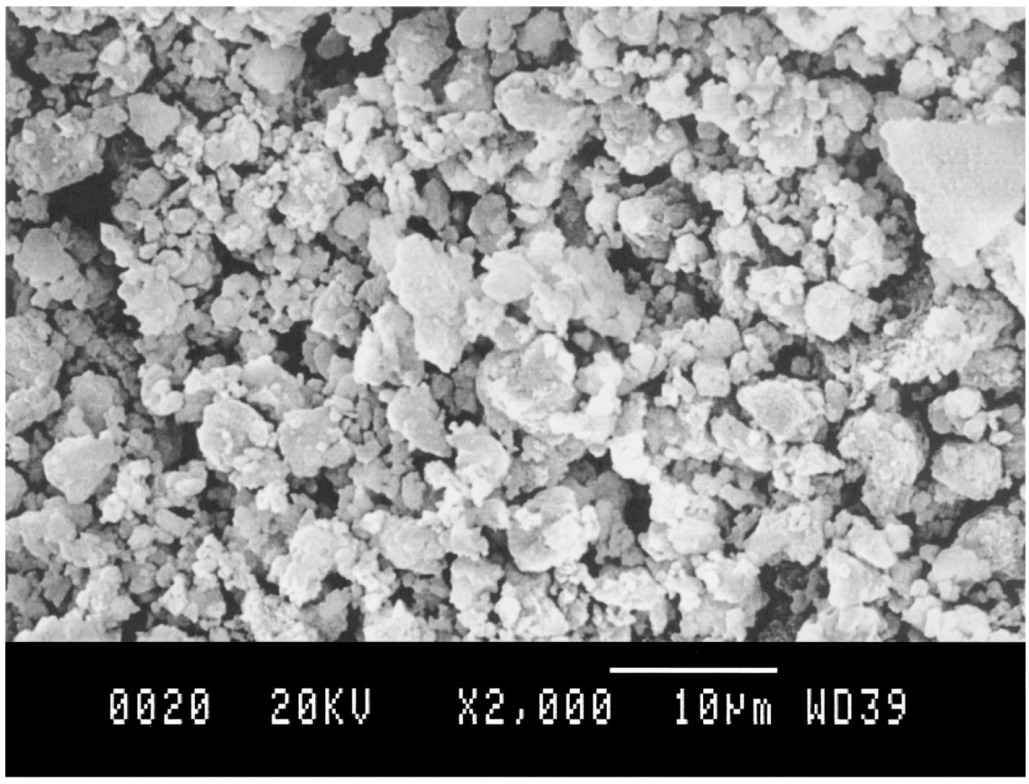

Figure 6 SEM picture of an $MgSiN_2$ powder synthesised at 1250 °C from a Si_3N_4 (SKW Trostberg)/Mg (Merck) starting mixture.

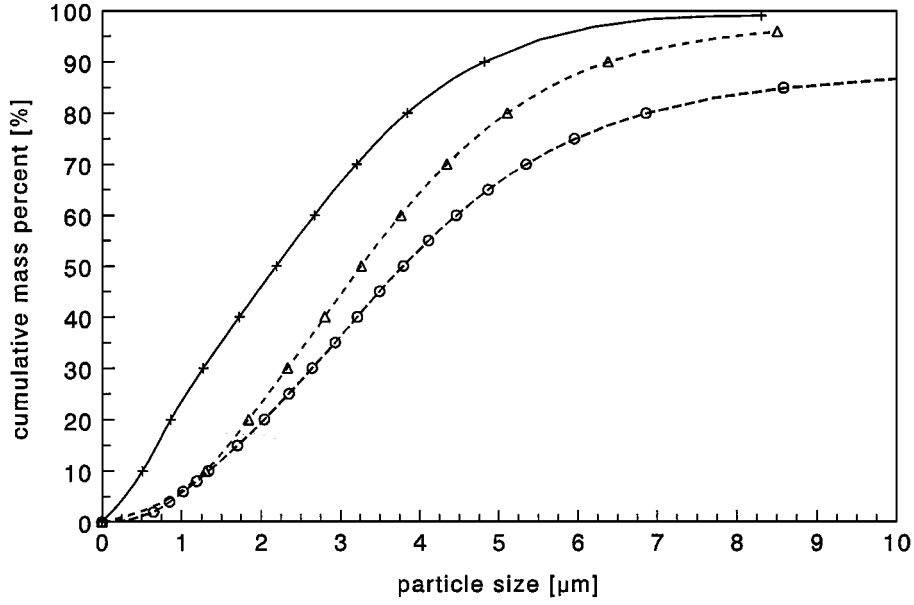

Figure 7 The particle size distribution as determined by Sedigraph measurements of Si_3N_4 (SKW Trostberg) starting material (+) and $MgSiN_2$ powder prepared thereof with Mg_3N_2 (Alfa) (△) or Mg (Merck) (o).

broader particle size distribution and a somewhat larger median particle size. In Fig. 7 the mass cumulative particle size distribution of the Si_3N_4 powder (SKW Trostberg), and the $MgSiN_2$ powders synthesised thereof with Mg_3N_2 (Alfa) and Mg (Merck) at 1250 °C are presented. As can be seen in Fig. 7 the starting Si_3N_4 powder has a narrow particle size distribution and a median particle size of 2.2 μm. The $MgSiN_2$ powder synthesised from the Mg_3N_2/Si_3N_4 starting mixture has also a narrow particle size distribution but the powder is coarser. The median particle size equals 3.2 μm. The $MgSiN_2$ powder prepared from the Mg/Si_3N_4 starting mixture has a broad particle size distribution but the median particle size, viz. 3.8 μm, is only slightly larger than the powder synthesised from the Mg_3N_2/Si_3N_4 starting mixture. The powder consisted partially of hard agglomerates, that could not be removed by ultrasonic treatment and are probably related to the formation of free Si metal during the synthesis.

For the $MgSiN_2$ powders two different morphologies were observed (Figs 8 and 9). The first one showed equiaxed grains with a primary particle size smaller than 3 μm and agglomerates smaller than 10 μm. The second one consisted of large porous sponge like agglomerates (~100 μm). The observed type of morphology was independent of the α/β ratio of the starting Si_3N_4

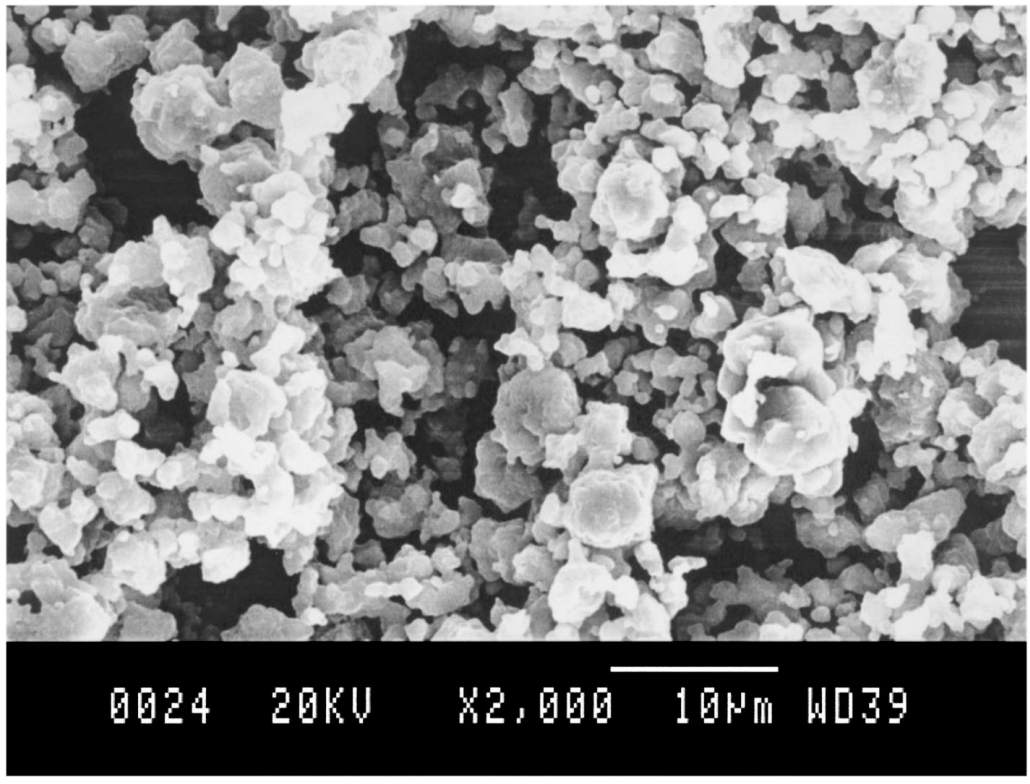

Figure 8 SEM picture of an $MgSiN_2$ powder synthesised at 1250 °C from a Si_3N_4 (HCST)/Mg (Merck) starting mixture.

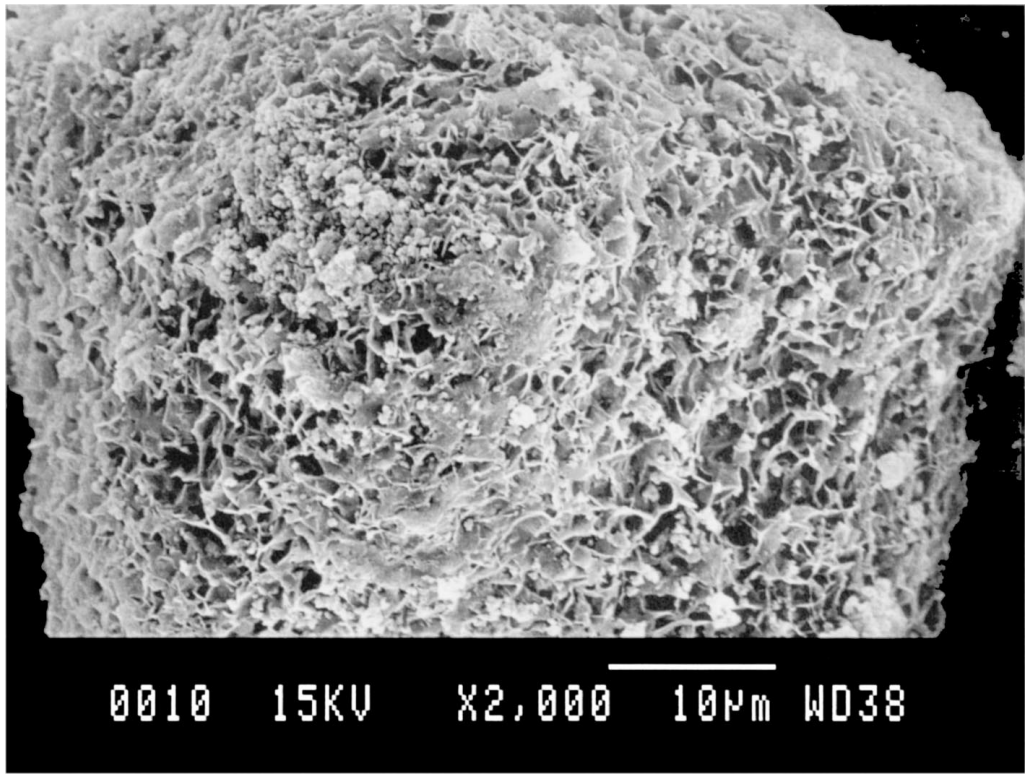

Figure 9 SEM picture of an $MgSiN_2$ powder synthesised at 1250 °C from an Si_3N_4 (Tosoh)/Mg_3N_2 (Alfa) starting mixture.

powder used and whether a Mg/Si_3N_4 or Mg_3N_2/Si_3N_4 starting mixture was used. If the Si_3N_4 starting powders of Tosoh or Ube were used then the sponge like $MgSiN_2$ particles were observed. If the Si_3N_4 starting powders of HCST and SKW Trostberg were used then small equi-axed $MgSiN_2$ particles were observed. For comparison the morphology of the Si_3N_4 starting material of HCST and Tosoh was investigated with the SEM. The Si_3N_4 powder of HCST consisted out of small grains whereas the Tosoh powder consisted out of large agglomerates of small grains. This indicates that the morphology of the Si_3N_4 starting material determines the morphology of the resulting $MgSiN_2$ powder.

3.6. Oxidation behaviour of $MgSiN_2$ powders

TGA/DTA measurements and furnace experiments in combination with XRD were used to study the oxidation behaviour of $MgSiN_2$. TGA/DTA experiments show that $MgSiN_2$ powders are oxidation resistant in air till 830 °C. At higher temperatures 4 reaction peaks are observed (Fig. 10); 3 exothermic peaks at 904, 1082 and 1362 °C, and 1 endothermic peak at 1459 °C. The

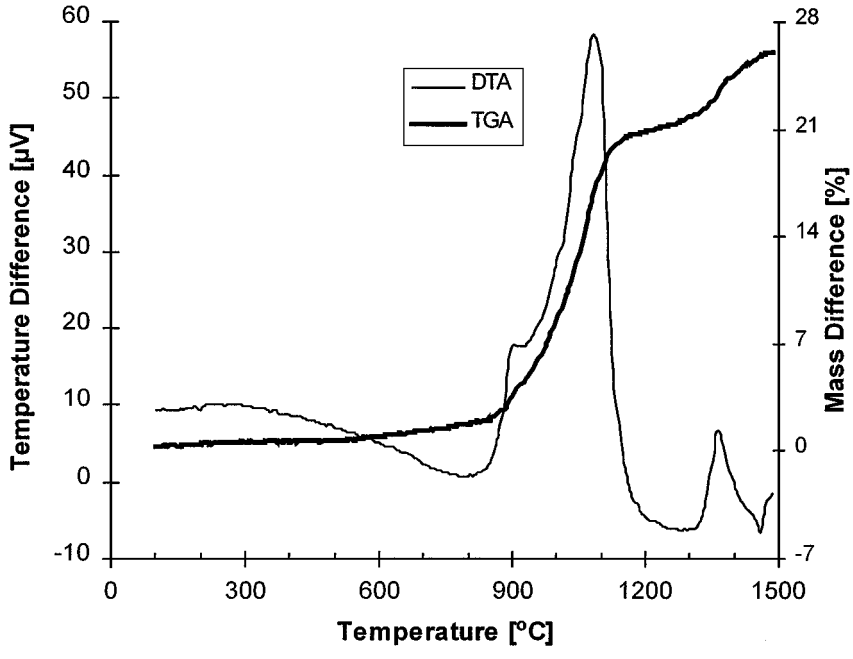

Figure 10 TGA/DTA plot of the oxidation behaviour of $MgSiN_2$ powder in air.

total weight gain for the first 2 DTA peaks is about 18 wt %. This mass gain can be represented by the following overall reaction:

$$2MgSiN_2 + 2\tfrac{1}{2}O_2 \rightarrow Mg_2SiO_4 + Si_2N_2O + N_2(+18.6\,wt\,\%)$$

The total weight gain after the third DTA peak is about 25 wt %. This can be represented by the following overall reaction:

$$2MgSiN_2 + 3O_2 \rightarrow Mg_2SiO_4 + SiO_2 + 2N_2(+24.8\,wt\,\%)$$

So after the third DTA peak the $MgSiN_2$ powder is totally oxidised. This peak is related to the fast oxidation of Si_2N_2O to SiO_2. The reaction temperature of about 1362 °C is in favourable agreement with the temperature mentioned in the literature [23] for the fast oxidation of Si_2N_2O powder at about 1330 °C. So the oxidation of $MgSiN_2$ is a two step process as shown by the TGA/DTA measurements. The fourth DTA peak at about 1459 °C is an endothermic one and is related to the phase transformation of SiO_2 from tridimite to cristobalite (1477 °C as deduced from Fig. 5 of Ref. [24]).

The isothermal oxidation behaviour of $MgSiN_2$ powder was studied in air, just above the oxidation temperature, at 850 °C. From the isothermal oxidation study it was clear that $MgSiN_2$ can be totally oxidised at 850 °C indicating that the intermediate reaction products are not stable. No parabolic oxidation behaviour was observed probably due to a superposition of the two above mentioned oxidation reactions.

4. Conclusions

The phase formation study of $MgSiN_2$ showed that nearly single phase $MgSiN_2$ powders can be obtained from Mg_3N_2/Si_3N_4 or Mg/Si_3N_4 mixtures. However, the reaction paths are different as shown with TGA/DTA. Oxygen poor $MgSiN_2$ powders can be prepared, not only by the conventional synthesis route starting with Si_3N_4 and Mg_3N_2, but also by starting with Si_3N_4 and Mg in a flowing $N_2/(H_2)$ atmosphere. This alternative synthesis route has the benefit of a lower reaction temperature and the disadvantage of a more critical processing due to the formation of free Si metal during the synthesis.

When using the standard synthesis temperature of 1250 °C, the overall oxygen content obtained for the $MgSiN_2$ powders varied between 0.9 and 6.1 wt % O, mainly determined by the oxygen content of the Si_3N_4 starting material. The lattice parameters of these powders do not depend on the overall oxygen concentration indicating that the maximum solubility of oxygen in the lattice is surpassed in accordance with the observed presence of some residual MgO. Its concentration in these powders suggest that the maximum solubility of oxygen in the $MgSiN_2$ lattice does not exceed 0.6 ± 0.2 wt %. By using improved processing conditions it is possible to synthesise powders with an oxygen content of only 0.1 wt % O. However, even in these powders containing only 0.1 wt % O some MgO could be detected with XRD indicating that the maximum solubility of oxygen in the $MgSiN_2$ lattice is even much lower than 0.6 wt %.

The study of the $MgSiN_2$ powders with SEM and the sedimentation method showed that the morphology of the $MgSiN_2$ powders is most probably determined by the morphology of the used Si_3N_4 starting material. If the starting Si_3N_4 powder was agglomerated, large sponge like $MgSiN_2$ particles were observed.

Oxidation experiments showed that $MgSiN_2$ powder is oxidation resistant in air till 830 °C as determined by TGA/DTA. At two different temperatures (1082 and 1362 °C) fast oxidation takes place indicating that the oxidation of $MgSiN_2$ is at least a two step process. An isothermal oxidation experiment at 850 °C showed that $MgSiN_2$ could be fully oxidised indicating that the intermediate oxidation products are not stable.

Finally it can be concluded that it is possible to synthesise $MgSiN_2$ powders with a very low oxygen content which are very suitable for further processing to ceramics with optimum thermal properties.

Acknowledgements

The authors would like to thank P. Gerharts, P. van Dijk and R. Kemps for their experimental contributions, G. Bezemer for the thermal analysis and particle size distribution measurements, A. Jonkers, P. Krüsemann and J. Hanssen (Philips Research Laboratories) for the determination of the oxygen and nitrogen content with the LECO gas analyser, M. Hendrix and H. Heijligers for their assistance with the SEM measurements, K.-J. Best of SKW Giesserei-Technik GmbH for providing the Silzot HQ Si_3N_4 powder.

References

1. A. ROOSEN, in "Electroceramics IV, Aachen (FRG) 1994," Vol. 2, edited by R. Waser, S. Hoffmann, D. Bonnenberg and Ch. Hoffmann (Augustinus Buchhandlung, Aachen), p. 1089.
2. C.-F. CHEN, M. E. PERISSE, A. F. RAMIREZ, N. P. PADTURE and H. M. CHAN, *J. Mater. Sci.* **29** (1994), 1595.
3. G. A. SLACK, *J. Phys. Chem. Solids* **34** (1973) 321.
4. W. A. GROEN, M. J. KRAAN and G. DE WITH, *J. Eur. Ceram. Soc.* **12** (1993) 413.
5. H. T. HINTZEN, W. A. GROEN, P. SWAANEN, M. J. KRAAN and R. METSELAAR, *J. Mater. Sci. Lett.* **13** (1994) 1314.
6. G. A. SLACK, R. A. TANZILLI, R. O. POHL and J. W. VANDERSANDE, *J. Phys. Chem. Solids* **48** (1987) 641.
7. H. T. HINTZEN, R. BRULS, A. KUDYBA, W. A. GROEN and R. METSELAAR, in Ceramic Transactions, Int. Conf. Ceram. Proc. Sci. Techn., Friedrichshafen (FRG), September 1994, edited by H. Hausner, G. L. Messing and S. Hirano (American Ceramic Society, Westerville, 1995) Vol. 51, p. 585.
8. H. T. HINTZEN, R. BRULS and R. METSELAAR, in Fourth Euro-Ceramics, Faenza (Italy), October 1995, edited by C. Galassi (Gruppo editoriale Faenza editrice S.p.A.) Vol. 2, p. 289.
9. J. DAVID and J. LANG, *C. R. Acad. Sc. Paris* **261** (1965) 1005.
10. Refcel, Calculation of Cell Constants and Calculation of All Possible Lines in a Powder Diagram by H. M. Rietveld, October 1972.
11. J. DAVID, Y. LAURENT and J. LANG, *Bull. Soc. Fr. Minéral. Cristallogr.* **93** (1970) 153.
12. B. D. CULLITY, "Elements of X-Ray Diffraction," 2nd ed. (Addison-Wesley, 1978).

13. N. MATTER, A. RIEDEL and A. WASSERMANN, *Mater. Sci. Forum* **133–136** (1993) 39; W. Pfeiffer and M. Schulze, *ibid.* **133–136** (1993) 45; G. Petzow and R. Sersale, *Pure and Appl. Chem.* **59** (1987) 1673; C. P. Gazzara and D. R. Messier, *Ceram. Bull*. **56** (1977) 777.
14. T. MURATA, K. ITATANI, F. S. HOWELL, A. KISHIOKA and M. KINOSHITA, *J. Amer. Ceram. Soc*. **76** (1993) 2909.
15. I. S. GLADKAYA, G. N. KREMKOVA and N. A. BENDELIANI, *J. Mater. Sci. Lett*. **12** (1993) 1547.
16. M. BARSOUM, P. KANGUTKAR and M. J. KOCZAK, *J. Amer. Ceram. Soc*. **74** (1991) 1248.
17. R. MULLER, Konstitutionsuntersuchungen und thermodynamischen Berechnungen im system Mg, Si/N, O, PhD dissertation, University of Stuttgard, 1981, p. 107.
18. R. J. BRULS, H. T. HINTZEN and R. METSELAAR, Preparation and Characterisation of $MgSiN_2$ Ceramics, to be published.
19. J. DAVID, *Rev. Chim. Miner*. **9** (1972) 717.
20. M. WINTENBERGER, F. TCHEOU, J. DAVID and J. LANG, *Z. Naturforsch*. **35b** (1980) 604.
21. Powder Cell, Programm zur Manipulation von Kristallstrukturen und Berechnung der Röntgenpulverdiffraktogramme. Werner Kraus, Dr. Gert Nolze, Bundesanstalt für Materialforschung und -prüfung 12205 Berlin Unter den Eichen 87 (1995).
22. S. WILD, P. GRIEVESON and K. H. JACK, *Spec. Ceram*. **5** (1972) 289.
23. J. PERSSON, P. O. KÄLL and M. NYGREN, *J. Amer. Ceram. Soc*. **75** (1992) 3377.
24. M. HILLERT, S. JONSSEN and B. SUNDMAN, *Z. Metallkd*. **83** (1992) 648.

Received 15 May
and accepted 23 December 1998